Environmental Technology & Innovation 32 (2023) 103274

Contents lists available at ScienceDirect

Environmental Technology & Innovation

journal homepage: www.elsevier.com/locate/eti

Application of long-chain ammonium polyphosphate to control inorganic fouling in agricultural saline water distribution systems

Changjian Ma [a,b], Jaume Puig-Bargués [c], Xuejun Wang [a], Renkuan Liao [d], Lili Zhangzhong [e], Zhaohui Liu [a], Yang Xiao [b,*], Yunkai Li [b]

[a] Shandong Academy of Agricultural Sciences, Jinan 250100, China
[b] College of Water Resources and Civil Engineering, China Agricultural University, Beijing 100083, China
[c] Department of Chemical and Agricultural Engineering and Technology, University of Girona, Girona 17003, Spain
[d] Key Laboratory of Simulation and Regulation of Water Cycles in River Basins, China Institute of Water Resources and Hydropower Research, Beijing 100048, China
[e] National Engineering Research Center for Information Technology in Agriculture, Beijing 100097, China

ARTICLE INFO

Article history:
Received 26 May 2023
Received in revised form 30 June 2023
Accepted 1 July 2023
Available online 6 July 2023

Keywords:
Ammonium polyphosphate
Drip irrigation
Emitter clogging
Fouling
Crystal structure

ABSTRACT

The inevitable inorganic fouling in saline water drip irrigation systems (SWDIS) with phosphorus fertilizer has become key obstacle for utilizing saline water and phosphate fertilizer. This study developed a greener anti-fouling method by intelligently applying a superior fertilizer (i.e. ammonium polyphosphate, APP). X-ray diffractions and Rietveld refinement method were used to determine the mineral composition and cell parameters of scales. Results showed that APP effectively minimized the inorganic fouling in SWDIS, with the fixed scales quantity reduced by 17.8–59.3%. Consequently, the average discharge and fertigation uniformity of SWIDS in APP groups were 26.4–49.5% and 40.5–63.5% higher than that in no-fertilizer groups. The aragonite and calcite contents were decreased by 52.9–63.7% and 35.3–53.3% with APP application, which was because of APP chelating salt cations (e.g., Ca^{2+}) to decrease the probability of carbonates formation. In addition, APP increased the cell volumes of aragonite and calcite to 0.26–5.33A^3, which resulted in the retrogression of crystallinity and phase purity. Moreover, compared with lower concentration with long time fertigation mode, the scales' contents in higher concentration with shorter time fertigation mode reduced by 20.9%. This study proposes an effective, eco-friendly fertigation method to control the inorganic fouling in SWDIS, which provide a new perspective for the sustainable management of saline water and phosphorus fertilizer in arid areas.

1. Introduction

The scarcity of freshwater resources has become the most challenges to agricultural irrigation in arid regions (Qin et al., 2019; Yu et al., 2019). Saline water widely distributed in arid regions, its amount is equivalent to freshwater (Rozema and Flowers, 2008). Hence, the use of saline water for irrigation would be an effective measure to alleviate the freshwater scarcity. However, due to saline water has active salts, the key problems associated with saline water

* Corresponding author.
E-mail address: xiaoyang@cau.edu.cn (Y. Xiao).

https://doi.org/10.1016/j.eti.2023.103274

irrigation are the negative impacts on plants and salts accumulation in soil (Jalali, 2007). Therefore, suitable methods for saline water application in arid regions has received increasing attentions.

Another key factor restricting sustainable agricultural development in arid areas is the low use efficiency of fertilizer, particularly for phosphorus (P) fertilize. The P fertilizer is easy to be fixed in the soil to form P fixation (unavailable form) when the soil moisture content is insufficient, resulting in the seasonal use efficiency of P fertilizer will not be higher than 25% (Syers et al., 2008; Wang and Chu, 2015; Xiao et al., 2023). The term P fixation is used to describe reactions that remove available phosphate from the soil solution into the soil solid phase (Sharma et al., 2013). There are two types of reactions (a) phosphate sorption on the surface of soil minerals and (b) phosphate precipitation by free Al^{3+} and Fe^{3+} in the soil solution. It is for this reason that soil P becomes fixed and available P levels have to be supplemented on most agricultural soils by adding chemical P fertilizers (Sharma et al., 2013), and even more, farmers usually increase the intensity of P fertilizer to meet the needs of crop growth (Zhao et al., 2020), which greatly increased the agricultural non-point source pollution (Ashley et al., 2011). Thus, it is necessary to improve the utilization efficiency of P fertilizer in arid regions.

Drip irrigation is one of the water-saving technology, which offers the opportunities to solve the utilization of saline water, and increase to use efficiency P fertilizer in arid areas. On one hand, drip irrigation could effectively reduce the soil salinity in the root zone of crops, thereby reducing the stress effect of soil salinity (Dehghanisanij et al., 2006). On the other hand, in drip irrigation systems, phosphate is directly transported to the crops root zone along with water, consequently increasing the migration distance (Ayars et al., 2017), and utilization efficiency of phosphate fertilizer by 25.4%–70.4% when compared with basic phosphorus fertilizer application (Shedeed et al., 2009; Mohammad et al., 2004; Rubeiz et al., 1989). However, due to the extremely narrow channel of the emitter (the core component of drip fertigation system) is only 0.5–1.2 mm, the phosphate application through drip fertigation has been challenging on a large scale. Haynes (1985) reported, the phosphate fertilizer easily reacts with Ca^{2+} and other cations in irrigation water and cause emitter inorganic clogging. The emitter inorganic clogging would directly reduce the fertigation uniformity and fertilizer utilization efficiency, and even reduce the operation life of drip irrigation systems. To make things worse, the combination of saline water and P fertilize could significantly aggravated the inorganic clogging issue.

In fact, many scholars have done a lot of research on the inorganic clogging of the emitter. As early as 1979, drip irrigation experiments using Colorado River irrigation water on citrus trees in south-western Arizona were conducted to evaluate clogging of emitters (Gilbert et al., 1979), and Gilbert found that inorganic chemical clogging substances played an important role in the emitter clogging. Hills et al. (1989) found that inorganic chemical fouling was the reason for reducing the uniformity of drip irrigation and the clogging mechanism was a gradual buildup of precipitate in the emitter's passage rather than an instantaneous obstruction. In recent years, the research on inorganic clogging in drip irrigation system has also made some progress. Liu et al. (2023) found that when no fertilizer and inorganic fertilizer were applied, the clogging substances in the emitter were inorganic fouling including precipitate fouling (i.e., calcite, aragonite and monohydrate calcite), particulate fouling (muscovite, feldspar, silica and chlorites). Shi et al. (2022) summarized the category, mechanism, and controlling methods of chemical clogging in drip irrigation system. So far, the inorganic fouling mitigation in saline water drip irrigation system (SWDIS) has been usually achieved through application such as hydrochloric acid (Hao et al., 2018). However, the use of chemicals are becoming restricted because of their negative impacts on the soil and crops, storing and handling risks, and high costs (Mercier et al., 2016; Wang et al., 2019). Thus, alternative greener, convenient and inexpensive anti-fouling technologies for SWDIS is in urgent need.

The latest research progress observed the fouling behavior in emitters are closely associated with different type of fertilizer (Shen et al., 2022). Previous studies have found the type of fertilizers could influence emitter clogging (Yang et al., 2019). In addition, the clogging behavior, such as clogging substance, clogging rates, were differed obviously with different concentrations of fertilizer (Xiao et al., 2020). The varying behavior of inorganic fouling highlighted, finding out an appropriate application mode of fertilizers might provide a new concept for inorganic fouling control in SWDIS. To date, the main phosphate fertilizers used in agricultural production are calcium sulfate and other traditional phosphate fertilizers, often having high risk of emitter clogging. For fertigation via drip irrigation systems, the fertilizers must be completely soluble and free of impurities. Typically, the sources of P recommended for drip irrigation are Monopotassium phosphate (MKP), Monoammonium phosphate (MAP), and Phosphoric acid. Recently, the achievements in the fertilizer industry offer a promising solution to address the risk of inorganic fouling in saline water P drip fertigation systems. A superior type fertilizer, i.e. Ammonium Polyphosphate (APP), has attracted great attention for its potential ability in mitigating inorganic fouling (Hasson et al., 2011; Xu et al., 2013). Previous literatures demonstrated that most polyphosphates do not easy to react with cations (e.g. Ca^{2+} and Mg^{2+}) in water to form precipitates under certain conditions, so they are often used as scale inhibitors. Similarly, APP is likely to act as scale inhibitors and phosphate fertilizers in SWDIS. However, the anti-fouling efficiency of APP fertilizer and its suitable application modes in SWDIS has not been yet explicitly understand.

Accordingly, the objectives of this study were to: (1) define the anti-fouling capacity of APP in SWDIS; (2) clarify the mechanism of APP reducing the risk of emitter clogging; (3) propose a suitable anti-fouling application mode of APP in SWDIS. Here, couple of open field identical SWDIS simultaneously operated was used to culture inorganic fouling with three concentrations APP. X-ray diffraction (XRD) and Rietveld refinement methods were applied to determine the composition and the lattice parameters of scales.

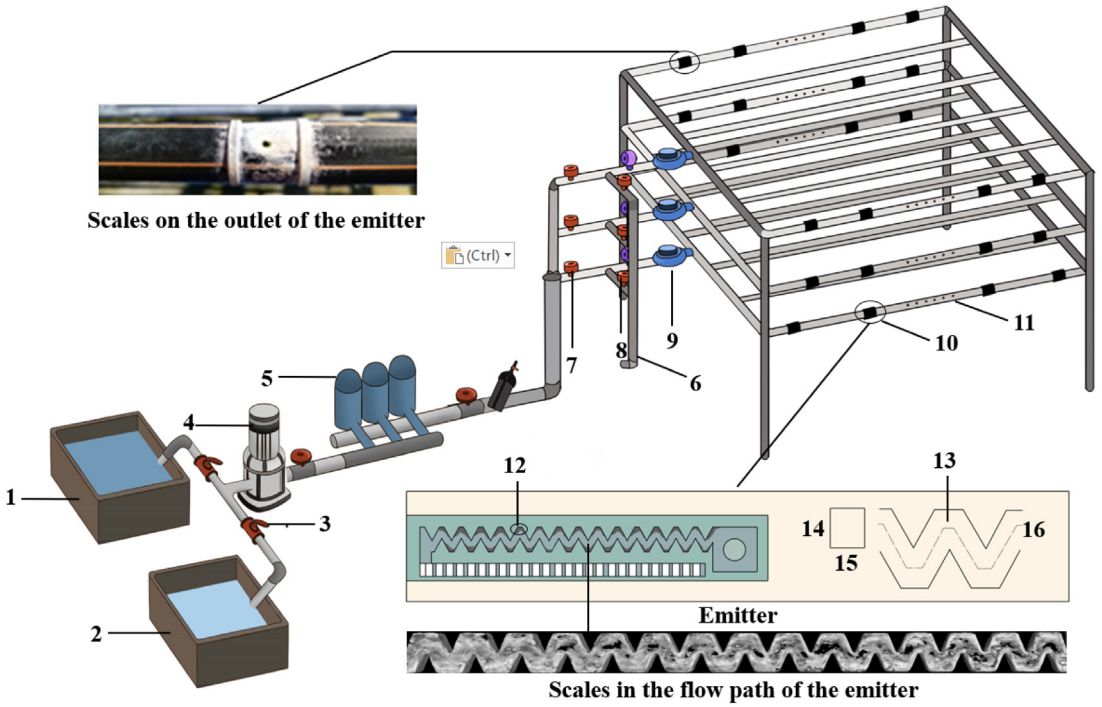

1-Fertigation source, 2-Water source, 3-Butterfly valve, 4-Water pump, 5-Disc filter (100 μm),

6- Precise adjusting valve, 7- Pressure gauge, 8- Flowmeter, 9- Pipes, 10-Drip emitter, 11-Drip lateral, 12-Scales,

13-Labyrinth channel, 14-Height, 15-Depth, 16-Length

Fig. 1. Schematic layout of SWDIS.

2. Materials and methods

2.1. Experimental setup

The experiment was conducted at China Agricultural University Beijing Tongzhou Experiment Station (116°41′2. 31″E,39°42′6. 93″N). The drip irrigation test platform (Fig. 1) of this experiment consists of three layers, every test platform layer is equipped with one same kind of drip emitter, and every kind of drip emitter is provided with 5 repeats. Three different kinds of flat emitters (E1, E2 and E3) were used, and their detailed geometrical parameters were listed in Table 1. The length of each drip lateral was 18 m and the distance between the drip emitters is 30 cm. The experiment was carried out for a total of 40 days, and the pressure during system operation was 0.1 MPa. A saline ground water source was used for experiment. The applied water quality basic characteristics and after P fertilizer application are listed in Table 2. To ensure the experimental water quality did not change greatly, the water was changed every 2 days. In addition, the initial P concentration in experimental saline water was less than 0.81 mg/L, which could be ignored. As the source of P fertilizer, APP was applied at 0, 0.15 and 0.30 g/L, the fertilizer concentration levels based on general practice (Wang et al., 2020; Xiao et al., 2020; Kang et al., 2004; Rose et al., 1999). The treatments were marked as CK (control group), APP_0.15 and APP_0.30, respectively. Considering the actual irrigation and fertilization field applications, the system ran once 8 h a day with a total running time of 40 days, and the fertilization was carried out at every alternative day. The fertilization/irrigation plans (Fig. A1) included low concentration/long term (LCLT), high concentration/short term (HCST) and CK treatments.

2.2. Evaluation parameters of emitter performance

A three-layer structure flow-measuring trolley was applied to test the emitter flow rate of the drip irrigation system. Make sure that there was a small bucket placed on the trolley under each emitter. And then use a stopwatch (0.01s) for timing (5 min). Finally, use an electronic balance (10^{-3} g) to weigh the water in the small bucket. In addition, this study

Table 1
Geometrical parameters of emitters used during the experiment.

Emitter	Rated discharge (L/h)	Flow path dimensions (mm)			Discharge coefficient	Flow index	Cross-sectional area (cm^2)
		Length	Width	Depth			
E1	0.95	85.02	0.55	0.51	3.10	0.51	2.01
E2	1.40	47.01	0.56	0.55	4.90	0.51	1.41
E3	1.60	19.04	0.55	0.49	5.20	0.51	1.20

Table 2
Average ± standard deviation of saline water quality parameters.

Treatment	pH	Ca^{2+} (mg/L)	Mg^{2+} (mg/L)	Fe^{3+} (mg/L)	Mn^{2+} (mg/L)	TH (mg/L)	TDS (mg/L)	EC (μS/cm)
CK	7.5 ± 0.1	85 ± 4	84 ± 5	0.053 ± 0.002	0.12 ± 0.01	557 ± 9	1028 ± 30	1368 ± 41
APP_0.15	7.3 ± 0.1	83 ± 5	82 ± 4	0.046 ± 0.003	0.13 ± 0.01	545 ± 9	1052 ± 26	1395 ± 37
APP_0.30	7.1 ± 0.1	86 ± 3	83 ± 5	0.058 ± 0.002	0.10 ± 0.01	556 ± 8	1093 ± 32	1452 ± 46

Note: Water quality parameters were tested by Pony Testing International Group Co., Ltd., China. pH was measured using a pH meter. Ca^{2+}, Mg^{2+}, Fe^{3+} and Mn^{2+} were tested by inductively coupled plasma optical emission spectrometry. Total hardness (TH) is presented as mg/L $CaCO_3$, it was tested by titration. Total dissolved solids (TDS) were tested by gravimetry using an electric blast drying oven and analytical balance. Electrical conductivity (EC) was tested using a conductivity meter.

assumed the water density was 1000 kg/m^3. And the calculation methods for emitters' discharge (Q) of drip irrigation systems was the following equation (Zhou et al., 2019):

$$Q = \frac{3 \times (m_{wk} - m_k)}{50T} \tag{1}$$

Q: the emitters' discharge (L/h); T: the emitters' discharge measurement time (min); m_k: the weight of empty bucket (g); m_{wk}: the total weight of empty bucket and measured outflow of the emitter within time T (g).

Calculation methods for average discharge variation rate (*Dra*) of drip irrigation systems was as follows (Xiao et al., 2023; Li et al., 2019):

$$Dra = \frac{\sum_i^n \frac{q_i^t}{q_i^0}}{n} \times 100\% \tag{2}$$

q_i^0: initial discharge for emitter i (L/h); q_i^t: discharge at t hour for emitter i (L/h); n: total number of emitters along the lateral. In addition, sixty emitters were used to determine Dra.

The outflow uniformity of SWDIS was represented by Christiansen of uniformity (*CU*) (Shen et al., 2022; Christiansen, 1942):

$$CU = 100\left(1 - \frac{\sum_{i=1}^n |q_i - \overline{q}|}{n\overline{q}}\right) \tag{3}$$

q_i: the discharge of emitter i (L/h); $\overline{q}$: the emitters' discharge in a treatment (L/h); n: total number of emitters along the lateral.

Traditionally, *CU* of SWDIS should not be lower than 80% as the standard for safe operation of the system, marked as $CU_{0.8}$. In addition, sixty emitters were used to determine the CU.

2.3. Extraction and evaluation of scales

During the experiment, samples were taken five times (at 8, 16, 24, 32 and 40 days) for each treatment. Five emitters from each part (i.e., head, middle and tail) were cut in a lateral for each emitter type. Thus, a total of 15 emitter samples were collected for each emitter type at each sampling event, being placed in ziploc bags and stored in the refrigerator at 4 °C.

2.3.1. Dry matter sampling and testing methods

The obtained each emitter sampling event (containing 15 emitter samples) were dried at 70 °C. The emitter samples with fouling on them (DW_1) were weighed using a high precision electronic weight balance (accuracy 10^{-4} g). Hereafter, the emitter samples were placed in a plastic bag with a zip lock closure, added 20 mL of deionized water, and bags were placed inside of an ultrasonic cleaning bath (Granbo, China; type: GBS-GW1530; working power: 900 W; frequency: 40 KHz) for 65 min to completely eliminate the fouling. The cleaned and dried emitters were reweighed again to determine the DW_2. The difference between DW_1 and DW_2 was the total weight of fouling substance.

2.3.2. Mineral composition of scales evaluation

The mineral components in fouling were measured using an X-ray diffractometer (manufacturer: Bruker, Germany; type: D8-Advance). The obtained dried mixed solid phase scales of every experiment treatment were uniformly ground and subjected to X-ray diffractometer analysis and then obtain a scales diffraction pattern. The basic test condition of the scanning process were as follows: voltage 40 kV, current 40 mA, copper target, wavelength $\lambda = 0.15406$ nm. Topas software (Bruker Corp, USA) was used to analyze the scale samples and then obtain the mineral contents and composition. Besides, Rietveld refinement was performed by using GSAS (General Structure Analysis System) (Larsson and Von Dreele, 1994) with EXPGUI interface (Toby, 2001) to determine the unit-cell parameters of each mineral component. The GSAS uses the Rietveld method as a refining tool based on the calculation of square minimums until it reaches the best adjustment between the intensity of the diffraction pattern observed. The refinement parameters included the scale factor and 36 background terms in a linear interpolation function, and unit-cell dimensions. In addition, calculated parameters of X-ray diffraction pattern for GSAS are 15–75°, 2θ. The chemical clogging scales located at the exit of the emitter at the end of the experiment are shown in Fig. A2.

2.3.3. Test method for all components of scales in emitters

Because X-ray diffractometer cannot determine the amorphous component in the scales, so that the all components of scales in emitters were tested using Fourier transform infrared spectrometer (FTIR, manufacturer: PerkinElmer, USA; model: PE spectrum 400), cracking gas chromatography-mass spectrometer (GC–MS, manufacturer: Frontier, Japan; model: EGA/PY-3030D-GCMS-QP2010), energy spectrometer scanning electron microscope (SEM-EDS, manufacturer: Jeol, Japan; model: JSM-6510A). The full-component analysis spectrum is shown in Fig. A3.

2.4. Statistical analyses

Excel spreadsheets (Microsoft, USA) was used to calculate the basic data. The significant differences between different treatments were analyzed by Paired t-test. SPSS (ver. 23.0, IBM Analytics, USA) was used to analyze the regressions and statistical analyses. Structural equation modelling (SEM) was used to test the hypotheses about causal relationships between APP-mineral composition of scales and mineral composition of scales-*Dra*. SEM was constructed using AMOS v22.0 (IBM, USA) to evaluate the direct and indirect correlations between APP, mineral composition of scales and *Dra*.

3. Results

3.1. System performance, inorganic fouling formation and changing process of SWDIS

Fig. 2 shows *Dra*, *CU*, *Dw*, the correlations of *Dra*, *CU* and *Dw* between different treatments of SWDIS. The data from Fig. 2 a–b and c–b demonstrated that *Dra* and *CU* of APP treatments were significantly higher than CK treatment by 26.4–49.5% and 40.5–63.5%. $CU_{0.8}$ of APP_0.15 was 56.9% higher than CK. At the same time, the *Dra* and *CU* were also significantly ($p < 0.05$) different between both APP concentration levels. The *Dra* and *CU* of APP_0.30 group were 18.3% and 16.4% higher those in APP_0.15 group. Meanwhile, APP tended to reduce the scales growth inside SWDIS compared with CK treatment. After the application of APP, the total amount of scales at the end of the system operation time was significantly ($p < 0.05$) reduced by 27.8–59.3%. The significant differences in scales dry weight between different concentration levels are shown in Table A3. Compared with APP_0.15, the total dry weight of scales in APP_0.30 treatment significantly ($p < 0.05$) decreased by 20.9%.

3.2. Mineral composition, mineral component proportions and surface morphology of scales

Fig. 3 shows Rietveld refinement patterns (Rietveld refinement patterns for lateral tail sampling point are taken as an example, the rest are shown in Fig. A3), mineral component proportions and surface morphology of scales. And the full-component analysis spectrum is shown in Fig.A4. The X-ray diffraction and the full-component analysis revealed that the main mineral components in scales were quartz, aragonite, calcite, muscovite, alkali feldspar, chlorite and P and the proportion of each mineral component is shown in Fig. 3a. The mineral components in CK treatment were mainly aragonite and calcite, while the mineral components in APP treatment were mainly P, aragonite and calcite (Fig. 3b–d). Meanwhile, the surface morphology of CK treatment was granular, while APP was granular and flocculent precipitation (Fig. 3e).

3.3. Dynamic variation of mineral composition content in scales

The variation of scales mineral composition in SWDIS are shown in Fig. 4. The amount of aragonite and calcite contents in APP treatments were significantly ($p < 0.05$) lower than CK, but the result is really the opposite for muscovite, chlorite, anorthite, quartz and P. Compared with CK, both APP treatments (0.15 and 0.30 g/L) significantly ($p < 0.05$) reduced the content of aragonite and calcite by 82.5–93.5% and 60.5–72.3%, respectively. However, the contents of muscovite, chlorite, anorthite and quartz were significantly ($p < 0.05$) comparatively higher for APP than CK treatment (Fig. 4),

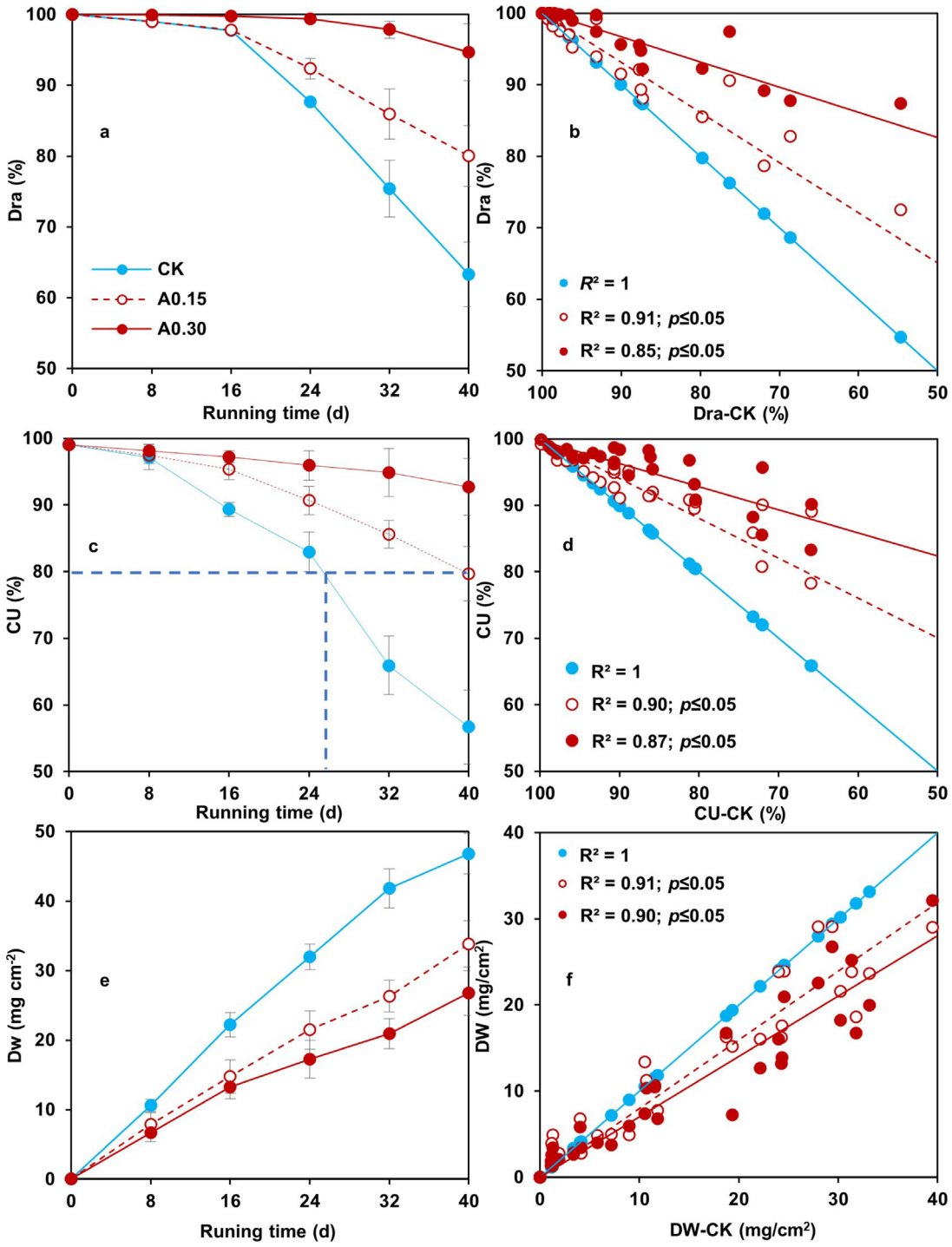

Fig. 2. System operation and inorganic fouling evaluation of SWDIS. Note: Fig a, c and e are *Dra* and *CU of SWDIS and* total dry weight (*Dw*) of scales, Fig b, d and f are the correlation of *Dra, CU* and D_w between APP and CK treatments. The *x* – axis of fig. b, d and e are the *Dra, CU* and D_w of CK treatments, the *y* - axis of fig. b, d and f are the *Dra, CU* and D_w across different treatments. $p < 0.05$ indicate that there are significantly difference between treatments.

and were increased significantly by 62.2–92.9%, 90.2–127.2%, 44.0–81.4%, 25.9–46.6%, and 174.2–623.3%, respectively. In addition, there was no P appeared in CK treatment during the whole experiment, but it was observed in both APP treatments. At the end of system operation time, P content in scales reached 8.1–10.4 mg/cm^2. Meanwhile, the content of scales mineral composition was also significantly ($p < 0.05$) different between both APP concentration levels. Thus,

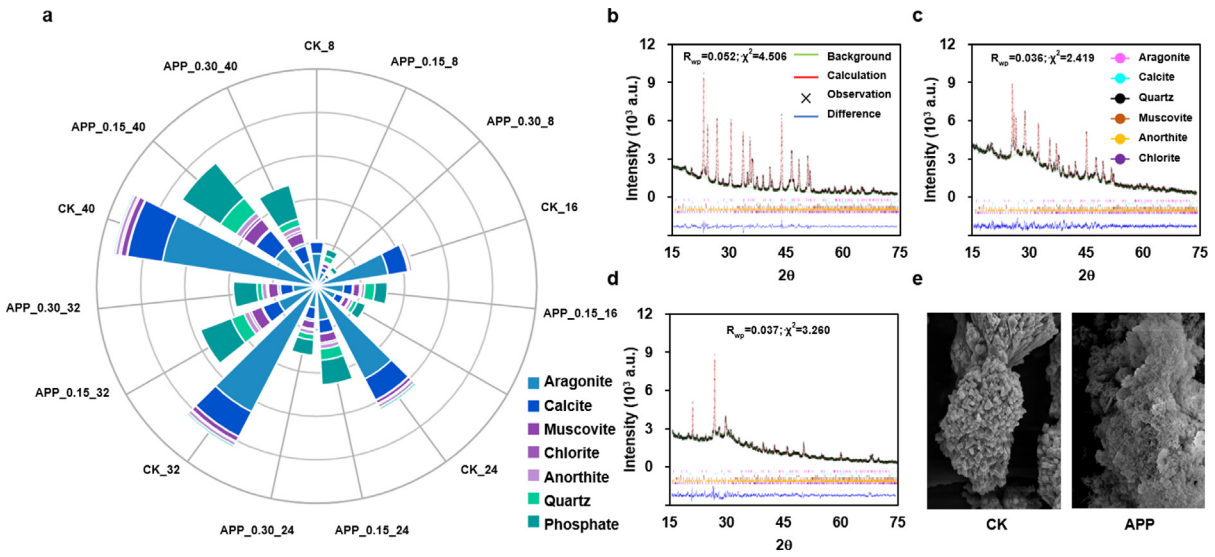

Fig. 3. Mineral composition, Rietveld refinement patterns and surface morphology of scales. Note: Fig a is mineral component proportions of scales. The treatments were marked as CK, APP_0.15 and APP_0.30 in materials and methods, the Numbers 8, 16, 24, 32 and 40 represent the running time of the system. For example, APP_0.15_8 represents the scales amount of APP_0.15 treatment at 8 days running time. Figs b–d are Rietveld refinement patterns of CK, APP_0.15 and APP_0.30 at 40d. Fig e is mineral surface morphology of scales.

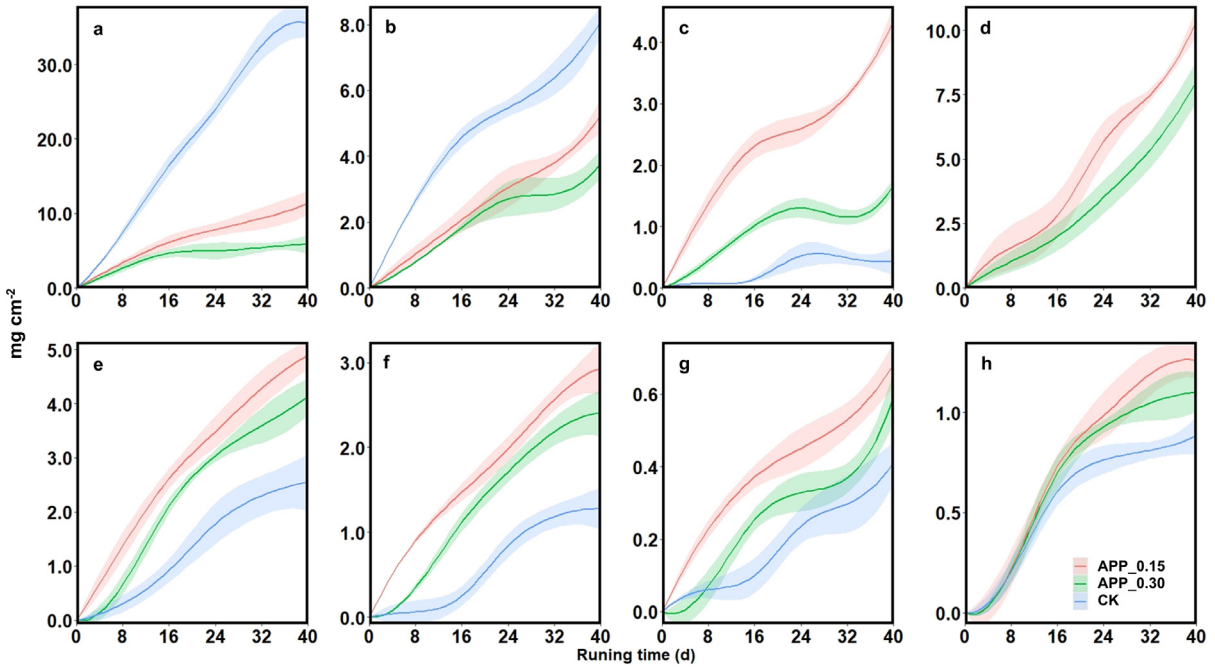

Fig. 4. Mineral component dry weight variation of scales. Note: Figs a–h are scales dry weight variation of aragonite, calcite, quartz, phosphate, silicate, muscovite, chlorite and anorthite.

APP_0.30 treatment reduced the aragonite, calcite, muscovite, chlorite, anorthite, quartz and P content by 20.6–48.4% and 22.9–27.8%, 17.9–51.7%, 13.1–31.9%, 12.5–24.6%, 61.7–68.0% and 19.3%.

3.4. Dynamic variation of unit-cell parameters in scales

The unit-cell parameters variations of aragonite, calcite, silicate (muscovite, chlorite, and anorthite), quartz scales in each treatment are shown in Fig. 5. Compared with CK treatment, the cell volume (Cv) of aragonite and calcite treated by

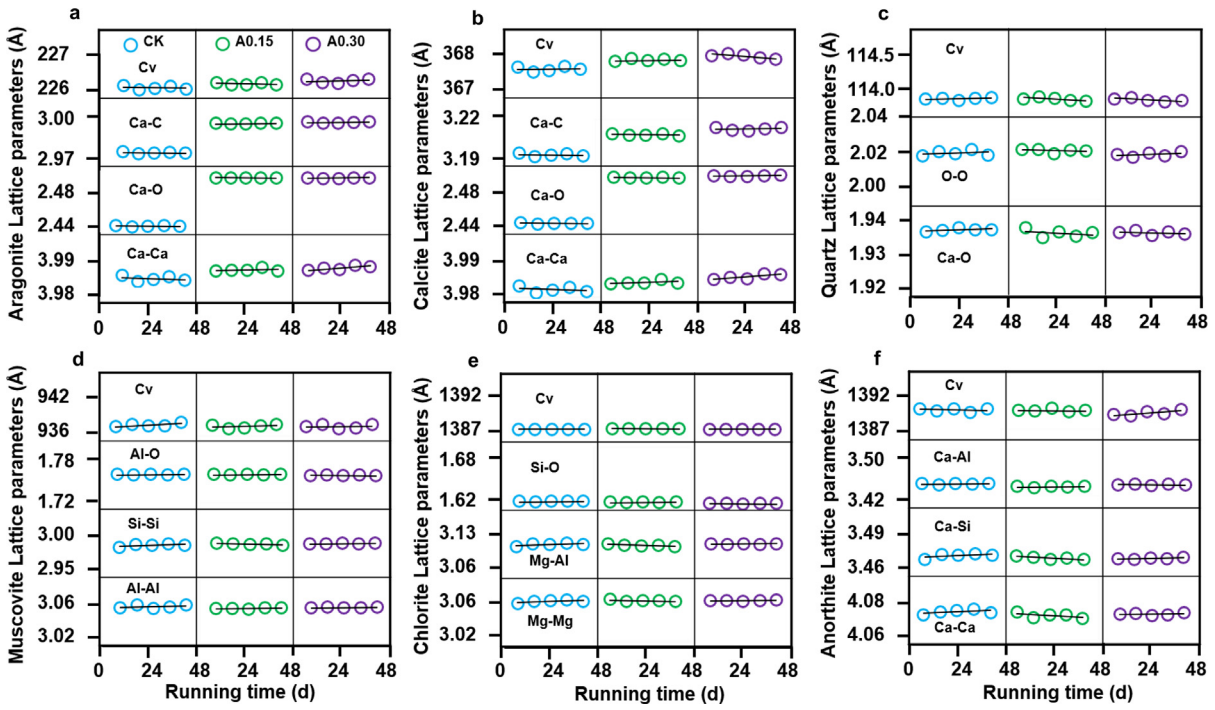

Fig. 5. Mineral component unit-cell parameters variation of scales. Note: Figs a–b are unit-cell parameters variation of aragonite and calcite. In Fig a, Cv is cell volume of mineral component, Ca–C, Ca–O and Ca–Ca are bond length (similarly hereinafter).

APP was significantly ($p < 0.05$) larger than that treated by CK, with an increase ratio of 0.26–0.48 and 3.32–5.33 A^3. Meanwhile, compared with CK treatment, the Ca–C, Ca–O and Ca–Ca bonds of aragonite and calcite in fertilization treatment all increased by 0.89–0.94%, 2.33–2.38%, 0.03–0.11% and 0.41–0.48%, 2.33–2.39%, 0.04–0.10%, respectively, and gradually increased with the increase of fertilizer concentration. But there was no significant difference in unit-cell parameters among the treatments of muscovite, anorthite, chlorite, and quartz. In addition, since the P of APP treatment is amorphous calcium, its unit-cell parameters cannot be determined by Rietveld refinement.

3.5. Correlation and SEM analysis between mineral composition content and Dra, CU,D_w

Correlation between mineral components of scales and *Dra, CU,* D_w was shown in Fig. 6 a. The results shown that the carbonate and silicate contents of all treatments were significantly ($p < 0.05$) negatively correlated with their *Dra and CU* of SWDIS and significantly ($p < 0.05$) positively correlated with D_w of emitter scales. And SEM analysis was conducted to further validate the hypothesis (Fig. 6). The results showed that APP presented negatively significant correlation with scales of aragonite and calcite, while positively significant correlation with dolomite, silicate, quartz and P. APP had the strongest direct effects on the aragonite whose standardized path coefficient reached −0.81 ($p < 0.001$), the second is calcite whose standardized path coefficient reached −0.76 ($p < 0.001$). The standardized path coefficient APP on silicate, P and quartz are 0.31, 0.65 and 0.59 ($p < 0.001$), respectively. Meanwhile, aragonite, calcite and P all had a significant negative effect on *Dra* (standardized path coefficient: −0.92, −0.60 and −0.31, $p < 0.001$), while silicate and quartz had no effect on *Dra*.

4. Discussion

4.1. Engineering application advantages and mechanism of APP in SWDIS

The results demonstrated that APP effectively increases the *Dra* and *CU* of SWDIS by reducing the D_w (Fig. 2) of scales in emitters, particularly the carbonate scales (Fig. 2). APP is a kind of long-chain mixture (Hagin and Lowengart, 1996; Waerstad and McClellan, 1976), so that it could chelate and shield some specific metal cations (e.g., Ca^{2+} and Mg^{2+}) in the solution at a certain concentration (Hagin and Lowengart, 1996; Noy and Yoles, 1979). The shielding effects of APP reduced the probability of anions reacting with metal cations (e.g., Ca^{2+} and Mg^{2+}) to form precipitates in saline water. On the other hand, the polyP causes the carbonate lattice to distort and therefore change the crystal morphology (Chew and Mat, 2015), which reduced the degree of crystallinity. Furthermore, the unit-cell parameters of crystals were

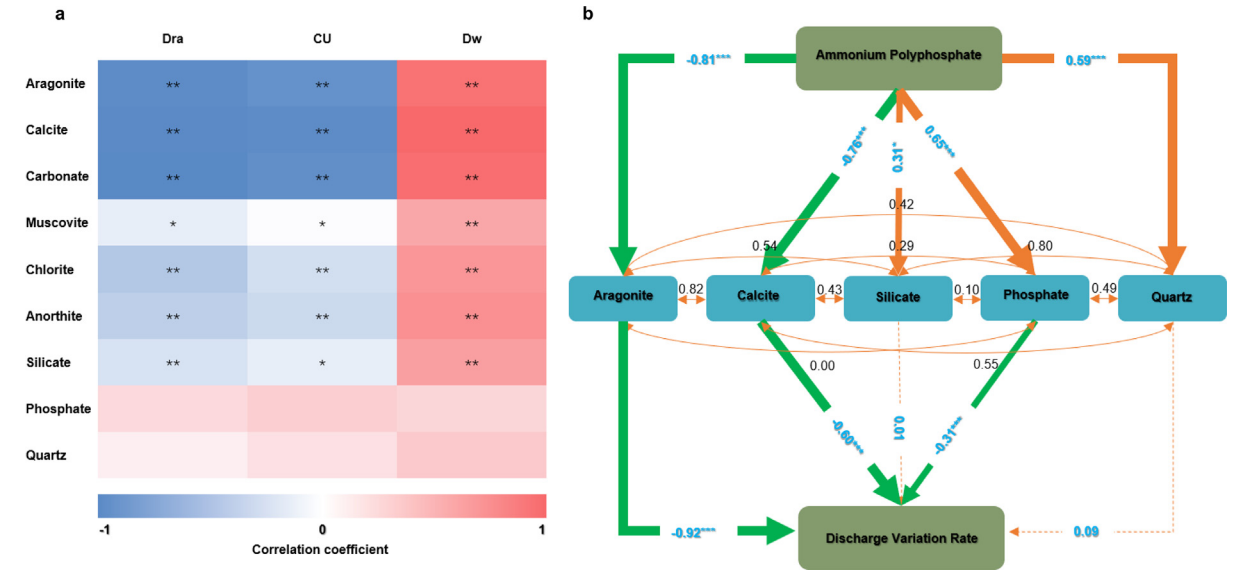

Fig. 6. Correlation and SEM analysis of the effect of APP on constituents of scales in *Dra* with saline water. Note: Figs a is correlation between Dra, CU, D_w and the mineral composition (aragonite, calcite, carbonate, muscovite, chlorite, anorthite, silicate, phosphate, quartz) for the different treatments. * and ** indicate the treatments are significantly different. Fig b SEM showed the relationship among fertilization treatment, mineral components of emitter scales and Dra. The initial independent variables were CK and APP treatment. Orange, dark gray and light gray radial lines respectively represented significant positive correlation ($p < 0.05$), significant negative correlation ($p < 0.05$) and no significant influence ($p > 0.05$). The orange and black lines between the mineral components represent the positive and negative interaction, respectively, and the numbers on the thin lines represent the standard path coefficient (β). The size of the number represents the strength of the correlation. . (For interpretation of the references to color in this figure legend, the reader is referred to the web version of this article.)

found to be related to the inorganic fouling (Hasson et al., 2011). Larger lattice parameters and bigger crystal volumes always indicate smaller binding energy among atoms, and then leading to further degradations of material properties, thus reducing the strength and stability of the material (Gao et al., 2011). In this study, the long-chain polymer in APP combines with water molecules to form hydrogen bonds (Yan et al., 2017), which increases the reaction probability of Ca^{2+} and HCO_3^- to form $CaCO_3$ (Liu et al., 2000). However, the overgrowth of crystal nucleus results in partial atomic vacancy inside the crystal nucleus (Gomez-Villalba et al., 2012), and other ions (e.g., Mn^{2+}, Fe^{2+}) in water will fill in the vacant position of crystal nucleus (Gomez-Villalba et al., 2012; Perdikouri et al., 2013). Since the ionic radius of these ions (e.g., Mn^{2+}, Fe^{2+}) are usually larger than calcium ions, which increased the crystal cell volumes of aragonite and calcite and create significant structural distortion, resulting in failure to form normal prism carbonate (Son et al., 2019; Saito et al., 2020). Furthermore, the increase of crystal cell volumes reduces the surface energy of crystals, thus reducing the probability of normal inorganic fouling of crystal nucleus caused by aragonite and calcite. Therefore, the increase of unit cell volume leads to the decrease of crystallinity and phase purity of scales (Wang et al., 2016; Zhang et al., 2014; Delacourt et al., 2006). The lower the crystallinity, the worse the stability of scales. Therefore, in this study, the carbonate scale was extremely unstable because of APP application, rendering it easier for the generated scales to drain out of emitter. Similarly, the increase of Ca–Ca, Ca–C and Ca–O bonds increased the volume of aragonite and calcite crystal cells (Fig. 5), and longer bonds will have a smaller binding energy (Gao et al., 2011). This reduces the internal density and hardness of crystals and leads to further degradation of material properties.

Overall, the anti-fouling effects of APP was mainly due to its special long chain structure, which can chelate Ca^{2+} and Mg^{2+}, and APP increased the size and crystallinity of carbonate crystal cells in saline water to destroy the phase purity of carbonate (Fig. 5). These two aspects together contributed to the significant reduction of aragonite and calcite (main mineral composition of scales) inorganic fouling, thus effectively increasing the SWDIS performance on *Dra* and *CU* (Fig. 2; Table A4).

4.2. Engineering application risks of APP in SWDIS

The application of APP in saline water increased the content of silicate, quartz and P scales, which may lead to a potential risk of emitter clogging and decrease the *Dra* and *CU* of SWDIS (Figs. 3 and 4). It is not caused by the variations in cell parameters, because the silicate (muscovite, chlorite, anorthite) and quartz mainly came from the precipitation and flocculation of solid particles in water sources (Liu et al., 2018; Zhou et al., 2018). The large number of cations in APP will attract the solid particles such as negatively-charged sediments in high saline water (Li et al., 2015; Zhou et al., 2019), and the resulting electrostatic effect makes the electric double layer structure continually compressed and thinner (Zhou

et al., 2019; Wang et al., 2005) to result in the flocculation and agglomeration of solid particles in the fertilizer solution (Liu et al., 2017). Coupled with the mutual adsorption of P anions and suspended particles in the solution, this process is further enhanced (Chen et al., 2015b). Overall, the application of APP could significantly change the water quality, altering the flocculation process, thus resulting in the increase of quartz, muscovite, chlorite, and alkaline feldspar (Figs. 3 and 4). The growth of P is mainly explained by the large amount of PO_4^{3-} in APP that inevitably reacted with Ca^{2+} in saline water to form calcium P precipitation (Ryan and Saleh, 1998), which caused a new increase of P scales. Furthermore, the scales of P, carbonate, silicate and quartz will interact with each other in a complex relationship (Wang et al., 2019; Xiao et al., 2020), which needs to be clarified by deep investigation in the future.

4.3. Engineering application proposals in SWDIS

In this experiment, it was found that the increase of silicate, quartz and other clogging substances in SWDIS leads to the decrease of the *Dra* and *CU* in the system. Both silicate and quartz come from saline water sources and solid particles can accelerate the coupling deposition of physicochemical scales (Liu et al., 2018). Therefore, improving the filtration accuracy of the water-fertilizer mixture and thus reducing the content of solid particles in the solution may help to reduce the content of silicate and quartz in the scales. However, the control threshold of total suspended solids in water-fertilizer mixture needs to be further tested and analyzed. In addition, increasing the frequency of lateral flushing would reduce the risk of silicate and quartz in the lateral entering the emitter passage (Puig-Bargués and Lamm, 2013), thus increasing the *Dra* and *CU* of SWDIS. Finally, higher fertilizer concentration of APP is more suitable for SWDIS. The higher the concentration of APP, the greater the effect in reducing crystallinity and phase purity of carbonate precipitates, thus inhibiting the process of carbonate inorganic fouling. And the degree of chelating for cations (e.g., Ca^{2+}, Mg^{2+}) can be enhanced by the higher APP concentration levels, which can reduce the probability of the contacts between scale-forming cations and anions, thus inhibited the carbonate and phosphate precipitation (Hagin and Lowengart, 1996; Hagin and Tucker, 1982).

APP has obvious advantages for agricultural application. Crops only absorb monovalent P in H_2PO_4 form (Bagyaraj et al., 2015). APP is a long-acting and slow-release fertilizer, which is gradually hydrolyzed to orthoP in soil and then efficiently absorbed by plants to improve the use rate of P (Ottman et al., 2006). Meanwhile, agricultural ammonium polyP is water high-solubility and slow-soluble (Chen et al., 2020; Do Nascimento et al., 2018), rendering it suitable for drip fertigation system. In addition, compared with conventional phosphate fertilizers such as monoammonium phosphate and diammonium phosphate, APP is not easy to react with calcium, magnesium and aluminum plasma in soil, which can increase the P use efficiency (Al-Dulaimi et al., 2021; Wang et al., 2021; Chen et al., 2015a). Besides, the APP long chain structure can chelate trace elements and improve the activity of trace elements such as zinc, manganese and copper (Gao et al., 2020; Mohammed and Abbas, 2015; McBeath et al., 2007). Furthermore, because of the high stability of APP, the elemental water-soluble fertilizer made from APP can avoid agglomeration, bulging bag, discoloration and precipitation of fertilizer (Xie et al., 2019). Of course, APP also has some disadvantages. The production of APP produces a lot of greenhouse gases such as carbon dioxide, which also has a negative impact on the environment (Eric and Céline, 2020). Finally, APP requires a lot of raw materials such as ammonia in the production process (Xu et al., 2022), and the price of ammonia itself fluctuates greatly, which will have a certain impact on the cost.

Although lots of meaningful findings were acquired from this study, some issues still are unaddressed and need to be investigated: (1) This study indicated that APP could effectively reduce the clogging problem of SWDIS, but the adaptability of APP to multiple types of water sources such as underground fresh water, river and lake surface water, and reclaimed water needs to be studied; (2) The adaptability of APP to different soil types and crop types also needs to be discussed.

5. Conclusion

(1) APP effectively increased *Dra*, *CU* and reduced the formation of scales and improved the hydraulic performance of SWDIS. *Dra* and *CU* of APP treatments was significantly ($p < 0.05$) higher than CK treatment by 26.4–49.5% and 40.5–63.5%, and the total amount of scales was significantly ($p < 0.05$) reduced by 27.8–59.3%.

(2) APP inhibits the inorganic fouling mainly by reducing the carbonate (aragonite and calcite) content, and the aragonite and calcite contents were decreased by 52.9–63.7% and 35.3–53.3%, respectively. In addition, APP increased the P, silicate, and quartz contents of scales, which may lead to a potential risk of emitter clogging.

(3) Compared to CK treatment, APP_0.15 increased the cell volume to 0.26–0.48 A^3, and enhanced the Ca–C, Ca–O, and Ca–Ca bonds of carbonate by 0.89–0.94%, 2.33–2.38%, and 0.03–0.11%, respectively. APP_0.30 increased the cell volume to 3.32–5.33 A^3, and enhanced the Ca–C, Ca–O, and Ca–Ca bonds of carbonate by 0.41–0.48%, 2.33–2.39%, and 0.04–0.10%, respectively.

(4) The mechanism of APP to alleviate chemical scales in SWDIS lies in two aspects: one is to decrease the probability of anions reacting with salt ions through chelation; the other is to increase the cell volumes of aragonite and calcite, rendering the retrogression of the crystallinity and phase purity of carbonate to reduce the formation of aragonite and calcite. The application of 0.3 g/L APP is a recommended strategy to alleviate the risk of inorganic fouling in SWDIS.

CRediT authorship contribution statement

Changjian Ma: Writing – original draft, Investigation, Formal analysis, Data curation. **Jaume Puig-Bargués:** Writing – review & editing. **Xuejun Wang:** Writing – review & editing. **Renkuan Liao:** Writing – review & editing. **Lili Zhangzhong:** Writing – review & editing. **Zhaohui Liu:** Visualization. **Yang Xiao:** Writing – review & editing, Investigation, Validation, Conceptualization, Methodology, Resources, Supervision, Project administration, Funding acquisition. **Yunkai Li:** Writing – review & editing, Conceptualization, Methodology, Resources, Supervision, Project administration, Funding acquisition.

Declaration of competing interest

The authors declare that they have no known competing financial interests or personal relationships that could have appeared to influence the work reported in this paper.

Data availability

Data will be made available on request.

Acknowledgments

We are grateful for the financial support from the Key R&D Plan of Shandong Province (2021CXGC010801, 2021CXGC010804), National Natural Science Foundation of China (52209074, 51790531, 51909007), National Key Research and Development Program of China (2021YFD1900900), and the Natural Science Foundation of Shandong Province, China (ZR2022QE079).

Appendix A. Supplementary data

Supplementary material related to this article can be found online at https://doi.org/10.1016/j.eti.2023.103274.

References

Al-Dulaimi, K.H., Farhan, K.J., Al-Falahi, M.N.A., 2021. Effect of ammonium polyphosphate application on NPK availability in soil and plant wheat growth. Int. J. Agric. Stat. Sci. 17 (2), 667–673.
Ashley, K., Cordell, D., Mavinic, D., 2011. A brief history of phosphorus: from the philosopher's stone to nutrient recovery and reuse. Chemosphere 84 (6), 737–746.
Ayars, J.E., Phene, C.J., Phene, R.C., Gao, S., Wang, D., Day, K.R., Makus, D.J., 2017. Determining pomegranate water and nitrogen requirements with drip irrigation. Agricult. Water Manag. 187, 11–23.
Bagyaraj, D., Sharma, M.P., Maiti, D., 2015. Phosphorus nutrition of crops through arbuscular mycorrhizal fungi. Current Sci. 108 (7), 1288–1293.
Chen, R., Liu, G., Zhong, W., Sun, W., Zhang, L., Hu, Z., Li, X., Chen, J., 2015a. Effect of ammonium polyphosphate on plant growth development and absorption of phosphorus and zinc in corn seedlings. Agric. Sci. Technol. 16 (8), 1716.
Chen, X.J., Zhang, C.L., Deng, S.L., Chen, Y.L., 2020. Conversion of ammonium polyphosphate (app) in acidic soil and its effect on soil phosphorus availability. Appl. Ecol. Environ. Res. 18, 4405–4415.
Chen, W., Zheng, H., Teng, H., Wang, Y., Zhang, Y., Zhao, C., Liao, Y., 2015b. Enhanced coagulation-flocculation performance of iron-based coagulants: effects of PO_4^{3-} and SiO_3^{2-} modifiers. PLoS One 10, e0137116.
Chew, C.B., Mat, R., 2015. The efficacy of calcium carbonate scale inhibition by commercial polymer scale inhibitors. Chem. Eng. Trans. 45, 1471–1476.
Christiansen, J.E., 1942. Irrigation by sprinkling. In: California Agricultural Experimental Station Bulletin, Vol. 670. University of California, Berkeley, California.
Dehghanisanij, H., Agassi, M., Anyoji, H., Yamamoto, T., Inoue, M., Eneji, A.E., 2006. Improvement of saline water use under drip irrigation system. Agricult. Water Manag. 85 (3), 233–242.
Delacourt, C., Poizot, P., Levasseur, S., Masquelier, C., 2006. Size effect of carbon-free $LiFePO_4$ powders: the key for superior energy density. Electrochem. Solid-State Lett. 9, 7.
Do Nascimento, C.A., Pagliari, P.H., Faria, L.d. A., Vitti, G.C., 2018. Phosphorus mobility and behavior in soils treated with calcium, ammonium, and magnesium phosphates. Soil Sci. Am. J. 82, 622–631.
Eric, W., Céline, V., 2020. Greenhouse gas emissions from inorganic and organic fertilizer production and use: a review of emission factors and their variability. J. Environ. Manag. 276, 111211.
Gao, H., Jiao, L., Peng, W., Liu, G., Yang, J., Zhao, Q., Qi, Z., Si, Y., Wang, Y., Yuan, H., 2011. Enhanced electrochemical performance of $LiFePO_4$/C via Mo-doping at fe site. Electrochim. Acta 56, 9961–9967.
Gao, Y., Wang, X., Shah, J.A., Chu, G., 2020. Polyphosphate fertilizers increased maize (Zea mays L.) P, Fe, Zn, and mn uptake by decreasing P fixation and mobilizing microelements in calcareous soil. J. Soils Sediments 20 (1), 1–11.
Gilbert, R.G., Nakayama, F.S., Bucks, D.A., 1979. Trickle irrigation: prevention of clogging. Trans. Asae 22 (3), 0514–0519.
Gomez-Villalba, L., López-Arce, P., Buergo, M.Alvarez.de., Fort, R., 2012. Atomic defects and their relationship to aragonite–calcite transformation in portlandite nanocrystal carbonation. Cryst. Growth Des. 12, 4844–4852.
Hagin, J., Lowengart, A., 1996. Fertigation for minimizing environmental pollution by fertilizers. Fert. Res. 43, 5–7.
Hagin, J., Tucker, B., 1982. Special fertilization practices and multinutrient fertilizers, in fertilization of dryland and irrigated soils. pp. 141–165.
Hao, F., Li, J., Wang, Z., Li, Y., 2018. Effect of chlorination and acidification on clogging and biofilm formation in drip emitters applying secondary sewage effluent. Trans. ASABE 61, 1351–1363.
Hasson, D., Shemer, H., A., Sher., 2011. State of the art of friendly green scale control inhibitors: a review. Ind. Eng. Chem. Res. 50, 7601–7607.
Haynes, R., 1985. Principles of fertilizer use for trickle irrigated crops. Fert. Res. 6 (3), 235–255.
Hills, D.J., Nawar, F.M., Waller, P.M., 1989. Effects of chemical clogging on drip-tape irrigation uniformity. Trans. Asae 32 (4), 1202–1206.

Jalali, Mohsen, 2007. Salinization of groundwater in arid and semi-arid zones: an example from Tajarak, western Iran. Environ. Geol. 52 (6), 1133–1149.
Kang, J.G., van Iersel, M.W., Nemali, K.S., 2004. Fertilizer concentration and irrigation method affect growth and fruiting of ornamental pepper. J. Plant Nutr. 27 (5), 867–884.
Larsson, A., Von Dreele, R., 1994. General Structure Analysis System. Los Alamos Laboratory, GSAS. Los Alamos, NM.
Li, K., Niu, W., Zhang, R., Liu, L., 2015. Accelerative effect of fertigation on emitter clogging by muddy water irrigation. Trans. Chin. Soc. Agric. Eng. 31, 81–90.
Li, Y., Pan, J., Chen, X., Xue, S., Feng, J., Muhammad, T., 2019. Dynamic effects of chemical precipitates on drip irrigation system clogging using water with high sediment and salt loads. Agricult. Water Manag. 213, 833–842.
Liu, Z., Ma, C., Xiao, Y., Zhangzhong, L., Muhammad, T., Li, Y., 2023. Application of chelated fertilizers to mitigate organic-inorganic fouling in brackish water drip irrigation systems. Water Manag. 285.
Liu, L., Niu, W., Wu, Z., Ayantobo, O.O., Guan, Y., 2018. Effect of fertilization and sediment flow hydraulic characteristics on emitter clogging in muddy water drip fertigation system. Irrig. Drainage 67, 713–723.
Liu, L., Niu, W., Wu, Z.G., Guan, Y., Li, Y., 2017. Risk and inducing mechanism of acceleration emitter clogging with fertigation through drip irrigation systems. Trans. Chin. Soc. Agric. Mach. 48, 228–236.
Liu, X., Tsukamoto, K., Sorai, M., 2000. New kinetics of $CaCO_3$ nucleation and microgravity effect. Langmuir 16, 5499–5502.
McBeath, T.M., Lombi, E., McLaughlin, M.J., Bünemann, E.K., 2007. Polyphosphate-fertilizer solution stability with time, temperature, and pH. J. Plant Nutr. Soil Sci. 170 (3), 387–391.
Mercier, A., Bertaux, J., Lesobre, J., Gravouil, K., Verdon, J., Imbert, C., Valette, E., Héchard, Y., 2016. Characterization of biofilm formation in natural water subjected to low-frequency electromagnetic fields. Biofouling 32, 287–299.
Mohammad, M.J., Hammouri, A., Ferdows, A.E., 2004. Phosphorus fertigation and preplant conventional soil application of drip irrigated summer squash. J. Agron. 3 (3), 162–169.
Mohammed, E.S., Abbas, S., 2015. Ammonium polyphosphate and ammonium orthophosphate as sources of phosphorus for Jerusalem artichoke. Alex. Sci. Exch. J. 36, 47–57.
Noy, J., Yoles, D., 1979. Precipitates formed by APP 11 — 37 — 0 in irrigation water. 59, 2129-2130..
Ottman, M.J., Thompson, T.L., Doerge, T.A., 2006. Alfalfa yield and soil phosphorus increased with topdressed granular compared with fluid phosphorus fertilizer. Agron. J. 98, 899–906.
Perdikouri, C., Piazolo, S., Kasioptas, A., Schmidt, B.C., Putnis, A., 2013. Hydrothermal replacement of aragonite by calcite: interplay between replacement, fracturing and growth. Eur. J. Mineral. 25, 123–136.
Puig-Bargués, J., Lamm, F.R., 2013. Effect of flushing velocity and flushing duration on sediment transport in micro-irrigation driplines. Trans. ASABE 56 (5), 1821.
Qin, Y., Mueller, N.D., Siebert, S., Jackson, R.B., AghaKouchak, A., Zimmerman, J.B., Davis, S.J., 2019. Flexibility and intensity of global water use. Nat. Sustain. 2 (6), 515–523.
Rose, M.A., Rose, M., Wang, H., 1999. Fertilizer concentration and moisture tension affect growth and foliar N, P, and K contents of two woody ornamentals. HortScience 34 (2), 246–250.
Rozema, J., Flowers, T., 2008. Ecology, crops for a salinized world. ENCE 322 (5907), 1478–1480.
Rubeiz, I.G., Oebker, N.F., Stroehlein, J.L., 1989. Subsurface drip irrigation and urea phosphate fertigation for vegetables on calcareous soils. J. Plant Nutr. 12 (12), 1457–1465.
Ryan, J., Saleh, M., 1998. Use of Phosphorus Fertilizers in Pressurized Irrigation Systems: Problems and Possible Solutions. Natural Resource Management Program. Alexandria University, Alexandria, Egypt.
Saito, A., Kagi, H., Marugata, S., Komatsu, K., Enomoto, D., Maruyama, K., Kawano, J., 2020. Incorporation of incompatible strontium and barium ions into calcite ($CaCO_3$) through amorphous calcium carbonate. Minerals 10, 270.
Sharma, S.B., Sayyed, R.Z., Trivedi, M.H., Gobi, T.A., 2013. Phosphate solubilizing microbes: sustainable approach for managing phosphorus deficiency in agricultural soils. Springerplus 2 (1), 587.
Shedeed, S.I., Zaghloul, S.M., Yassen, A., 2009. Effect of method and rate of fertilizer application under drip irrigation on yield and nutrient uptake by tomato. Ozean J. Appl. Sci. 2 (2), 139–147.
Shen, Y., Puig-Bargués, J., Li, M., Xiao, Y., Li, Q., Li, Y., 2022. Physical, chemical and biological emitter clogging behaviors in drip irrigation systems using high-sediment loaded water. Agricult. Water Manag. 270, 107738.
Shi, K., Lu, T., Zheng, W., Zhang, X., Zhangzhong, L., 2022. A review of the category, mechanism, and controlling methods of chemical clogging in drip irrigation system. Agriculture 12.
Son, S., Newton, A.G., Jo, K.N., Lee, J.Y., Kwon, K.D., 2019. Manganese speciation in Mn-rich $CaCO_3$: A density functional theory study. Geochim. Cosmochim. Acta 248, 231–241.
Syers, J.K., Johnston, A.E., Curtin, D., 2008. Efficiency of soil and fertilizer phosphorus use : reconciling changing concepts of soil phosphorus behavior with agronomic information. FAO Fert. Plant Nutr. Bull. 18.
Toby, B.H., 2001. EXPGUI, a graphical user interface for GSAS. J. Appl. Crystallogr. 34, 210–213.
Waerstad, K.R., McClellan, G.H., 1976. Preparation and characterization of some long-chain ammonium polyphosphates. J. Agricult. Food Chem. 24, 412–415.
Wang, J., Chen, L., Liu, L., Deng, X., 2005. Experimental study on effect of positively charged ion in river on the velocity of sediment particles. Adv. Water Sci. 16 (2), 169–173.
Wang, J., Chu, G., 2015. Phosphate fertilizer form and application strategy affect phosphorus mobility and transformation in a drip-irrigated calcareous soil. J. Plant Nutr. Soil Sci. 178 (6), 914–922.
Wang, F., Fang, Z., Y., Zhang., 2016. Polyethylene glycol-induced growth of $LiFePO_4$ platelets with preferentially exposed (010) plane as a cathode material for lithium ion battery. J. Electroanal. Soc. 775, 110–115.
Wang, X., Gao, Y., Hu, B., Chu, G., 2019. Comparison of the hydrolysis characteristics of three polyphosphates and their effects on soil phosphorus and micronutrient availability. Soil Use Manage. 35, 664–674.
Wang, Y., Xu, D., Yang, J., Yan, Z., Luo, T., Li, X., Zhang, Z., Wang, X., 2021. Determination and correlation of the Ca^{2+} and Mg^{2+} solubility in ammonium polyphosphate solution from 278.2 to 323.2 K. J. Chem. Eng. Data.
Wang, Z., Yang, X., Li, J., 2020. Effect of phosphorus-coupled nitrogen fertigation on clogging in drip emitters when applying saline water. Irrig. Sci. 38 (4), 337–351.
Xiao, Y., Ma, C., Li, M., Zhangzhong, L., Song, P., Li, Y., 2023. Interaction and adaptation of phosphorus fertilizer and calcium ion in drip irrigation systems: the perspective of emitter clogging. Agricult. Water Manag. 282, 108269.
Xiao, Y., Puig-Bargués, Jaume., Zhou, B., Li, Q., Li, Y., 2020. Increasing phosphorus availability by reducing clogging in drip fertigation systems. J. Clean. Prod. 262, 121319.
Xie, W., Wang, X., Li, Y., Xu, D., Zhong, Y., Yang, J., 2019. Simultaneous determination of various phosphates in water-soluble ammonium polyphosphate. Chromatographia 82, 1687–1695.

Xu, Y., Zhang, B., Zhao, L., Cui, Y., 2013. Synthesis of polyaspartic acid/5-aminoorotic acid graft copolymer and evaluation of its scale inhibition and corrosion inhibition performance. Desalination 311, 156–161.
Xu, D., Zhong, B., Wang, X., Li, X., Zhong, Y., Yan, Z., Yang, J., Li, X., Wang, Y., Zhou, X., 2022. The development road of ammonium phosphate fertilizer in China. Chin. J. Chem. Eng. 41 (1), 170–175.
Yan, H., Zhao, Z., Wang, Y., Jin, Q., Zhang, X., 2017. Structural modification of ammonium polyphosphate by DOPO to achieve high water resistance and hydrophobicity. Powder Technol. 320, 14–21.
Yang, X., Wang, Z., Li, J., Li, Y., Liu, H., Wang, J., 2019. Effect of phosphorus fertigation on clogging in drip emitters applying saline water. In: 2019 ASABE Annual International Meeting. American Society of Agricultural and Biological Engineers, p. 1.
Yu, Y., Pi, Y., Yu, X., Ta, Z., Sun, L., Disse, M., Zeng, F., Li, Y., Chen, X., Yu, R., 2019. Climate change, water resources and sustainable development in the arid and semi-arid lands of central Asia in the past 30 years. J. Arid Land 11 (1), 1–14.
Zhang, N., Lin, L., Xu, Z., 2014. Effect of synthesis temperature, time, and carbon content on the properties and lithium-ion diffusion of $LiFePO_4$/C composites. J. Solid State Electrochem. 18, 2401–2410.
Zhao, Y., Li, Y., Yang, F., 2020. Critical review on soil phosphorus migration and transformation under freezing-thawing cycles and typical regulatory measurements. Sci. Total Environ. 141614.
Zhou, H., Li, Y., Wang, Y., Zhou, B., Bhattarai, R., 2019. Composite fouling of drip emitters applying surface water with high sand concentration: dynamic variation and formation mechanism. Agricult. Water Manag. 215, 25–43.
Zhou, B., Wang, D., Wang, T., Li, Y., 2018. Chemical clogging behavior in drip irrigation systems using reclaimed water. Trans. ASABE 61, 1667–1675.